Characterization of the Marine Atmosphere for Free-Space Optical Communication

Linda M. Wasiczko[‡], Christopher I. Moore[‡], Harris R. Burris[§], Michele Suite[‡],
Mena Stell[§], James Murphy, G. Charmaine Gilbreath[‡],
William Rabinovich[‡], William Scharpf[‡]
[‡]US Naval Research Laboratory, 4555 Overlook Ave. SW, Washington, DC 20375
[§]Research Support Instruments, 4325-B Forbes Blvd, Lanham, MD 20706

ABSTRACT

The Chesapeake Bay Detachment of the Naval Research Laboratory (NRL-CBD) provides an ideal environment for characterizing the effects of the marine atmosphere on free space optical communication links. The site has recently been converted to an operational 10 mile (16.2 km) one-way test range to collect information on propagation statistics in a variety of atmospheric conditions. The results presented here compare the contributions of thermal gradients across the bay to the variations in intensity scintillations across the bay.

INTRODUCTION

The Lasercomm Test Facility (LCTF) at the Naval Research Laboratory's Chesapeake Bay Detachment provides a unique location to study atmospheric propagation in a maritime environment. The addition of the one-way testbed has greatly enhanced the capabilities of the range, while also providing many measurement challenges. The remote side of the range, located at Tilghman Island, MD, now houses equipment to characterize atmospheric turbulence, atmospheric transmission, angle-of-arrival fluctuations, bit error ratio, packet transmission statistics, and a variety of other atmospheric parameters. The data presented in this paper is an initial assessment of the performance of the angle-of-arrival monitor and the three aperture atmospheric parameter diagnostic (TAAPD). This is a continuously evolving process, and we expect measurement techniques to continue to improve in order to more completely characterize the performance of free space optical communication links in the maritime environment.

EXPERIMENTAL SETUP

The NRL-CBD Lasercomm test facility has recently been upgraded to a one-way propagation path across the Chesapeake Bay. Previously, results have been reported on our round trip propagation results, where an array of 25 solid retroreflectors located on a tower on NRL-Tilghman Island, MD folded the optical link back to the CBD facility on the western side of the Chesapeake Bay [1,5]. The conversion to a one-way propagation path allows for a more accurate characterization of the path because the angle-of-arrival and C_n^2 measurements are made along one direction. Additionally, the path is on a slant, which is representative of a large deck to small deck ship-to-ship or ship-to-shore lasercomm link is likely to be implemented at. The transmitter located at CBD is approximately 30 m above sea level, while the receiver for the one-way link is approximately 5 meters above sea level at Tilghman Island. Figure 1 is a pictorial representation of the NRL-CBD lasercomm test facility.

Report Documentation Page

Public reporting burden for the collection of information is estimated to average 1 hour per response, including the time for reviewing instructions, searching existing data sources, gathering and maintaining the data needed, and completing and reviewing the collection of information. Send comments regarding this burden estimate or any other aspect of this collection of information, including suggestions for reducing this burden, to Washington Headquarters Services, Directorate for Information Operations and Reports, 1215 Jefferson Davis Highway, Suite 1204, Arlington VA 22202-4302. Respondents should be aware that notwithstanding any other provision of law, no person shall be subject to a penalty for failing to comply with a collection of information if it does not display a currently valid OMB control number.

1. REPORT DATE **2006**	2. REPORT TYPE	3. DATES COVERED **00-00-2006 to 00-00-2006**

4. TITLE AND SUBTITLE **Characterization of the Marine Atmosphere for Free-Space Optical Communication**	5a. CONTRACT NUMBER
	5b. GRANT NUMBER
	5c. PROGRAM ELEMENT NUMBER
6. AUTHOR(S)	5d. PROJECT NUMBER
	5e. TASK NUMBER
	5f. WORK UNIT NUMBER

7. PERFORMING ORGANIZATION NAME(S) AND ADDRESS(ES) **Naval Research Laboratory,4555 Overlook Avenue, SW,Washington,DC,20375**	8. PERFORMING ORGANIZATION REPORT NUMBER

9. SPONSORING/MONITORING AGENCY NAME(S) AND ADDRESS(ES)	10. SPONSOR/MONITOR'S ACRONYM(S)
	11. SPONSOR/MONITOR'S REPORT NUMBER(S)

12. DISTRIBUTION/AVAILABILITY STATEMENT
Approved for public release; distribution unlimited

13. SUPPLEMENTARY NOTES

14. ABSTRACT

15. SUBJECT TERMS

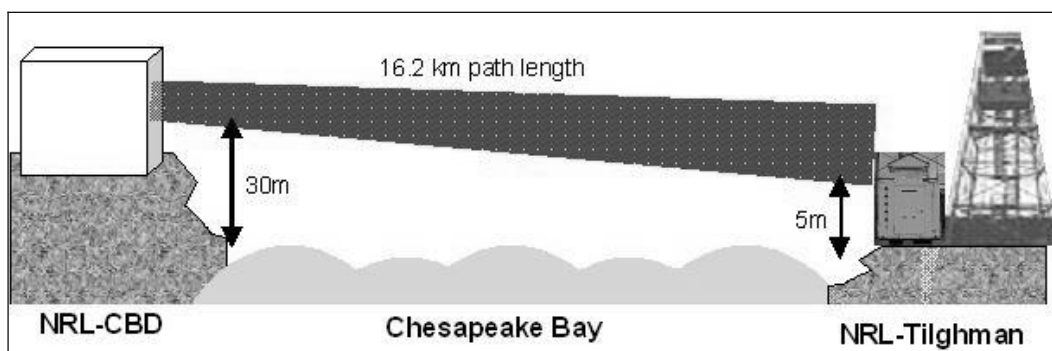| 16. SECURITY CLASSIFICATION OF:			17. LIMITATION OF ABSTRACT	18. NUMBER OF PAGES **12**	19a. NAME OF RESPONSIBLE PERSON
a. REPORT **unclassified**	b. ABSTRACT **unclassified**	c. THIS PAGE **unclassified**			

Fig. 1: NRL's Lasercomm Test Facility (LCTF). The transmitter is located at NRL-CBD on the western side of the Chesapeake Bay. The receiver is located at NRL-Tilghman Island on the top of the conex box. The retro-reflector array used in round-trip testing is still mounted on the tower at Tilghman approximately 15m above sea level.

The transmitter configuration implemented at the LCTF is a modification of a very reliable system we have used for our round trip experiments in the past. The transmitter's optical antenna consists of the output of a single mode fiber launched into a 4 inch Achromat ($f \approx 23$ cm). Beam steering is accomplished through the use of a 1 inch Newport Fast Steering Mirror (FSM) with a resolution of better than 1 μrad, and a range of ±1.5 degrees. The system may be set up for packet testing, bit error rate testing, or video transmission. The packet test configuration, shown in Fig. 2, uses a SC-connectorized, asymmetric Ethernet transmitter made by IMC Networks for 10/100 Ethernet transmission. The long haul unit has an output power of 0dBm in single-mode fiber. The output of the Ethernet transmitter is input to an INO EDFA preamplifier and then passed through a fiber optic isolator, so that the optical input power at the Keopsys EDFA is greater than 6 dBm. The Keopsys EDFA may be operated over a range of 19.5 dBm (preamp only) to 37 dBm. In clear low turbulence conditions, 19.5 dBm is more than enough power to close the 16.2 km one way link. In the future, an automated filter wheel will be installed on the transmitter to allow access to a wider range of transmitted power levels..
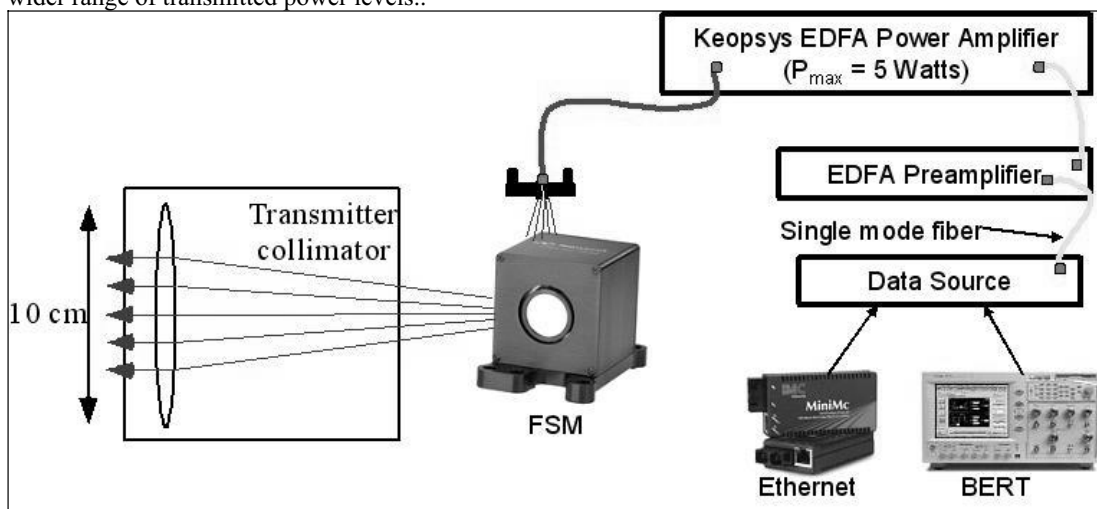

Fig. 2: Transmitter setup for lasercomm testing along the one-way link. In the Ethernet configuration, IMC Networks MiniMc transmitter is used as the data source. In the bit error rate testing setup, the Agilent 86130 or Anritsu ME522A BERT is used to generate a pseudorandom data stream.

The receiver system located at Tilghman Island consists of three subsystems that record various propagation statistics and communication metrics to assist in the characterization of the viability of free space optical communications in the maritime environment. Figure 3 is a photograph of the receiver subsystems located on the roof of the conex container. The angle-of-arrival monitor consists of a 5 inch Orion telescope with a Spiricon 1550-M phosphor-doped Si CCD camera in the image plane of the

telescope. The camera images are collected by a DBA systems video tracker for processing. The video tracker outputs the x and y components of the intensity centroid of the image at 60 Hz. This information is then sent to a 12-bit National Instruments A/D data acquisition card for subsequent processing. The variations in x and y of the centroid are used to determine the azimuthal, elevation, and radial components of the angle-of-arrival variance[1]. From these components, the refractive index structure function, C_n^2, may be estimated using the following relation[2]:

$$C_n^2 = \frac{\sigma_\beta^2 D^{1/3}}{2.91L} \quad \text{when } D >> \ell_o \qquad (1)$$

where D is the receiver aperture diameter, L is the propagation path length, ℓ_o is the inner scale of turbulence and σ_β^2 is the angle-of-arrival variance. The angle-of-arrival, β, is measured in radians. This design for an angle-of-arrival or passive turbulence monitor has previously been reported in Ref. 1. Using an incoherent source (i.e. a spotlight), scintillation readings from the angle-of-arrival monitor correlated with C_n^2 readings from a commercial scintillometer with a coefficient of 0.875. In the present one-way setup across the bay, the angle-of-arrival monitor is observing the fluctuations of a coherent source (i.e. the transmitted 1550 nm laser output). Since the angle-of-arrival monitor on the conex container is closer to the bay surface than the incoherent monitor, they sample different atmospheric paths and are not expected to correlate.
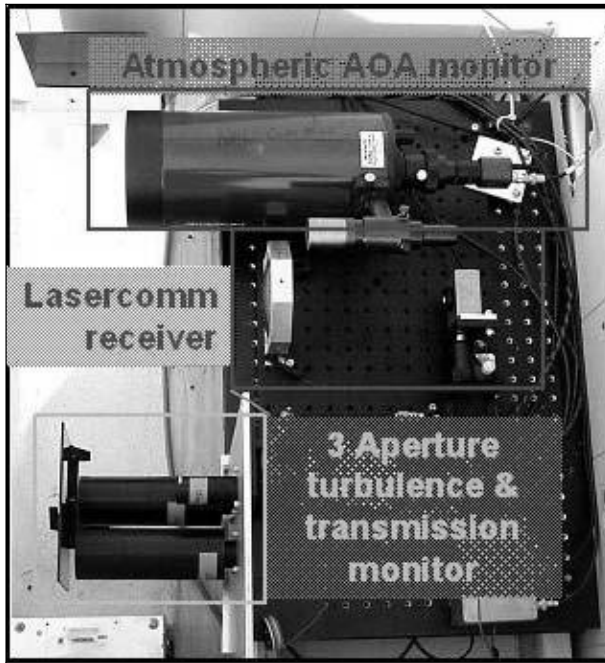

Fig. 3: The one-way across-the-bay receiver system. The system consists of an angle-of-arrival monitor (upper), a free space laser communications receiver (middle), and a three aperture atmospheric parameter diagnostic (TAAPD) (lower).

The lasercomm receiver uses another 4 inch Achromat to focus light on a 200 μm diameter Sensors Unlimited InGaAs APD detector, Model SU-001ATR with an integrated transimpedance amplifier (TIA) and automatic gain control (AGC). In the case that BER testing is conducted on the link, the electronic signal from the detector undergoes a clock recovery and data retiming using the Maxim 3270 CDR chip operating at 155 Mbps. The sensitivity of the receiver is specified as -43 dBm, although the measured sensitivity is -40 dBm. A thorough discussion of the lasercomm receiver is presented in Reference 3.

The third subsystem at Tilghman is the three aperture atmospheric parameter diagnostic (TAAPD). The TAAPD setup allows for the study of aperture averaging, C_n^2, and inner and outer scale[4]. The three apertures are InGaAs Pin photodiodes with aperture stops of 15mm, 32mm, and 50mm in front of the

lenses. The 32mm and 50mm apertures use 2 inch fast aspheres to focus light onto a 1 mm detector, while the 15mm aperture is a 1 inch f/2 spherical lens collecting light onto a 1 mm detector. Thorlabs lens tubes are also used to baffle the stray light, with 1 inch diameter lens tubes used on the 15mm aperture, and 2 inch diameter lens tubes used on the 32 mm and 50 mm apertures. Each aperture uses a Judson Technologies model J22TE2-66C-R01M InGaAs PIN photodetector with a responsivity of 0.9 A/W at 1550 nm and an integrated two-stage thermoelectric cooler. Each of the three detector signals is then preamplified using a Judson Technologies PA7 amplifier. The 32mm and 50mm signals were set to the medium gain of 10^6 V/A, while the small 15 mm aperture used a gain of 10^7 V/A. At the time of the measurements presented in this paper, each aperture was filtered directly in front of the detector with a 1 inch 1550nm bandpass filter with a 10.5 nm passband. During sunset, the DC background on the detectors steadily rises and corrupts the measurements on the 32mm and 50mm apertures, because the 1550 nm bandpass filters are extremely angle sensitive and do not reject light over the entire field of view of the two larger apertures. Also, the detectors look almost directly west and collect both direct sunlight and reflections from the water as the sun nears the horizon on clear days. The setup is undergoing modifications to improve the background light rejection by increasing the baffling length by 9 inches, and installing two inch 1500 nm longpass and 1550nm bandpass filters in front of the two inch receive lenses.

Receiver data at Tilghman is logged using a set of Labview programs. In order to facilitate alignment and data analysis, a variety of data is sent back from Tilghman to CBD using a Freewave 100 kbps RF Ethernet modem. Due to the bandwidth limitations imposed by the use of the RF modem, raw data is not read back from Tilghman Island. This forces part of the data analysis to be completed autonomously by a series of laptop computers located in the conex box at Tilghman.

For the three aperture setup, a Labview program logs data into three files, containing moments, a histogram, and one second averages. The three aperture moments file logs the mean, variance, skew (3rd moment), kurtosis (4th moment), the two next moments, and the maximum raw voltage for 1 minute time intervals of data sampled at 6 ksamples/second. A histogram is created from measured voltages over a one minute period. The 20 bins have widths based on the variation of voltages during the measurement period. The voltages are measured by a 16-bit National Instruments A/D card, with a resolution of 0.306 mV. The one-second averages and maximum readings over the 1 second interval are also continuously logged and transmitted back to CBD over the RF link.

Estimates of C_n^2 from the angle-of-arrival setup are logged every 10 seconds. The sensitivity of the angle-of-arrival monitor does not render accurate measurements over all receive power levels due to the low dynamic range of the CCD. Therefore, results using the AOA are only presented where applicable.

ATMOSPHERIC TURBULENCE IN THE MARITME ENVIRONMENT

We have previously reported that the maritime environment experiences severe vertical gradients along the Chesapeake Bay test range[5]. Typically, moderate to low turbulence conditions are observed across the LCTF range. Figures 4 a, b, and c are images taken during low, medium, and strong turbulence conditions across the bay. The strong turbulence observation, shown in Fig. 4c, is a state that occurs a few times during the year, typically during the spring and fall. Other interesting phenomena have been previously observed at the Chesapeake Bay test range, including mirages and double images[6].   Ref. 6 provides an extensive discussion on the relationship of near-surface optical refraction measurements to the near-surface temperature profile.
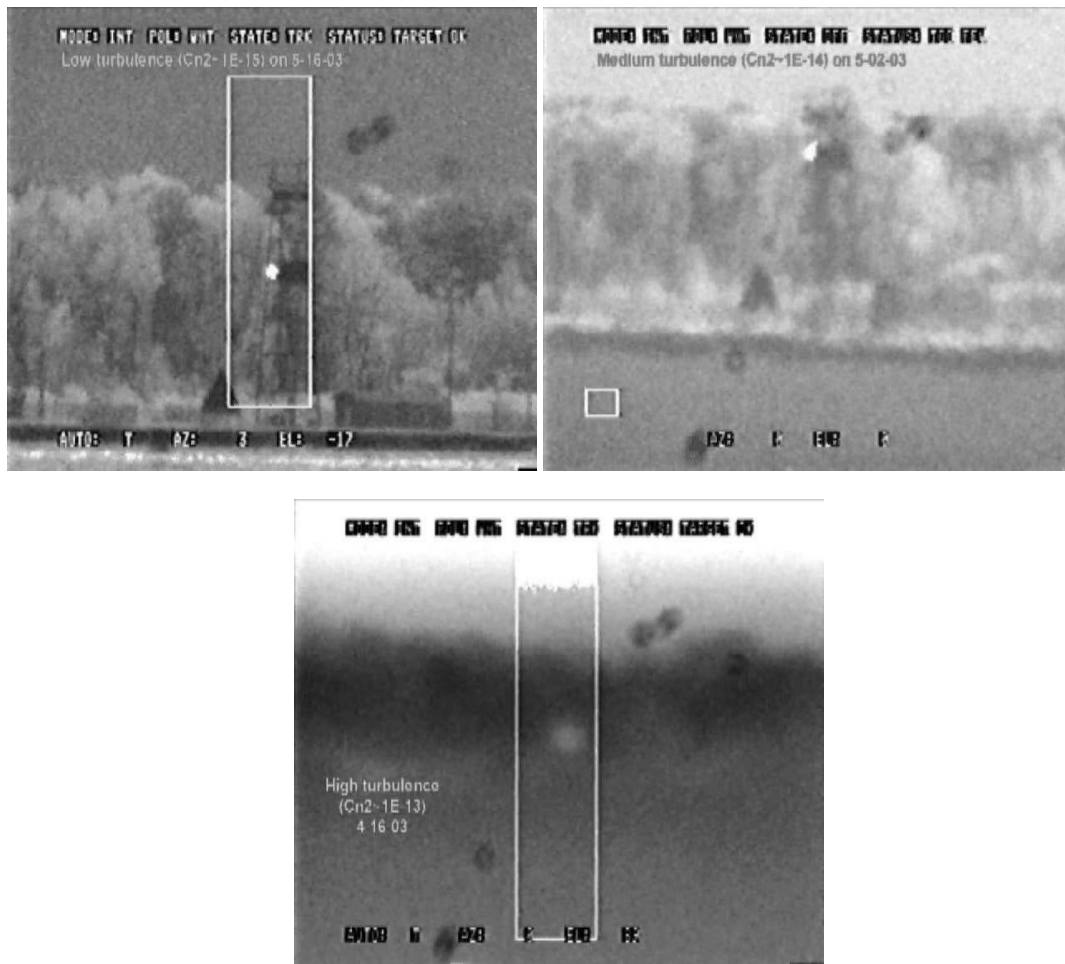
Fig. 4 a,b,c: Images of a tower at Tilghman Island, MD. The images were taken during conditions of low, medium, and strong turbulence (left to right, top to bottom, respectively).

The coherent angle-of-arrival monitor located on the conex container at Tilghman Island is not expected to correlate with the incoherent angle-of-arrival monitor located back at CBD, as previously mentioned. The coherent monitor samples a downward slant path, whereas the incoherent monitor is closer to horizontal since the spotlight is mounted well above the bay surface on the tower at Tilghman Island. It is not expected that the values will correlate. The scintillation should also appear stronger on the coherent monitor path since that monitor samples the stronger turbulent layers closer to the sea/land surface. Fig. 5 is a sample of C_n^2 measurements logged simultaneously on the coherent angle-of-arrival system and the incoherent turbulence monitor.
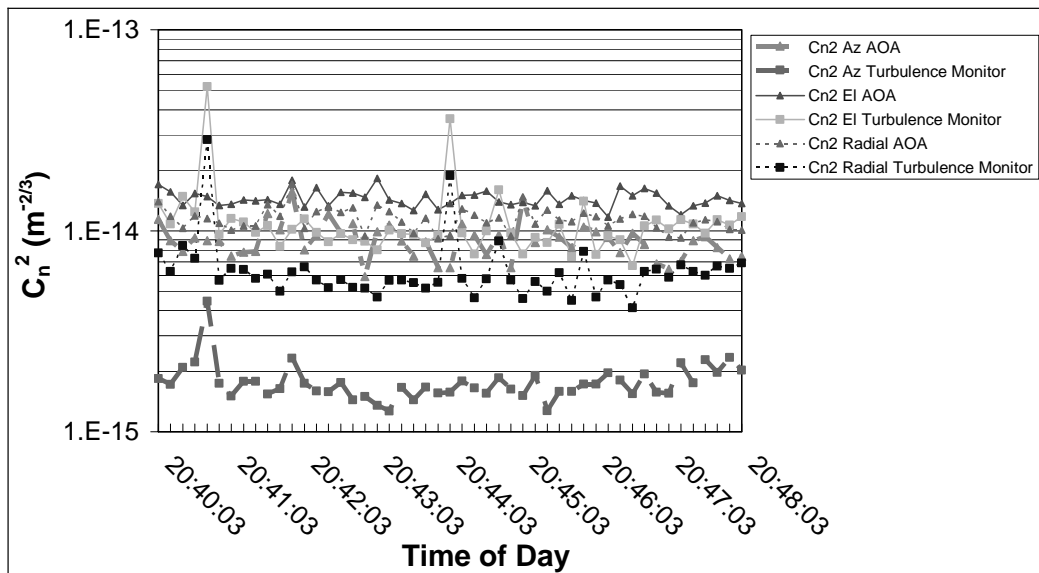
Fig. 5: Measurements of C_n^2 in the azimuthal, elevation, and radial directions using the coherent angle-of-arrival monitor (AOA) and the incoherent turbulence monitor.

Correlations of the azimuthal, elevation, and radial components of one-minute averages of C_n^2 measured from the coherent and incoherent turbulence monitor are apparent in Fig. 5. A calculation of the correlation coefficients over the entire measurement time for the azimuthal, elevation, and radial components of C_n^2 shows that the measurements are statistically independent, with correlation coefficients near 0. The uncertainty in the synchronization between the incoherent and coherent C_n^2 measurements contributes to a reduced dependence between the measurements; however the measurements should be statistically independent overall. The data in Fig. 5 for the coherent scintillometer was collected with a diverged transmitter beam (~500μrad). At this long propagation path length, this coherent scintillometer setup works well with a collimated or diverged beam, given sufficient power on the Spiricon CCD array.

The strong vertical refractive gradients across the bay are expected to cause significant fluctuations in the beam in elevation. Fig. 6 is a plot of the ratio of the azimuthal to the elevation deviations of the image as a function of collimation. From the data, the elevation fluctuations are approximately twice as strong as the azimuthal fluctuations. The level of fluctuations is also consistent across six different divergence angles. As the transmitter wave becomes more spherical wave-like, the amplitude of the fluctuations remains steady.
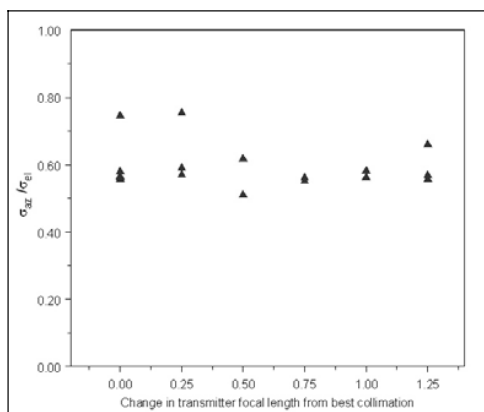

Fig. 6: Ratio of the fluctuations in the azimuthal to elevation components as a function of transmitter divergence.

THREE APERTURE ATMOSPHERIC PARAMETER DIAGNOSTIC (TAAPD)

The length of the Chesapeake Bay test range often precludes conventional atmospheric measurement equipment from being implemented. In conjunction with researchers from the University of Central Florida and the Defense Science and Technology Organization (DSTO) Australia, we have adapted a TAAPD configuration in the expectation of extracting information on three atmospheric parameters[4]. These parameters are C_n^2, the refractive index structure parameter, ℓ_o, inner scale, and L_o, outer scale. The setup may also be used for the study of aperture averaging.

In the first iteration of the three aperture setup, we have written a Labview program to log mean and maximum voltage levels from each of the apertures at 1 second intervals. As previously stated, the amount of information we can log is constrained by the RF bandwidth of our Tilghman Island to CBD link. The mean and maximum voltage data was initially used for the alignment of the three apertures on the across the bay link. Alignment, baffling, and filtering are extremely important to the quality of the data acquired from the three apertures. Nearly 6 inches of standard Thorlabs lens tubes are used for baffling on each aperture, and are seen in Fig. 3. As mentioned previously, 1 inch 1550nm bandpass filters provide some filtering in front of the detector, however the bandpass filter rejection is optimal only over a narrow angular range, which is narrower than the field of view. The three detectors have a wide field of view, and the limited baffling and filtering on the 32 mm and 50 mm apertures is unable to restrict this FOV to a level sufficient enough to remove the impact of the background light level on the measurements. Due to the fact that the receivers look nearly due west, prior to sunset on clear sunny days, background levels in the 100s of mV are observed on the 32mm and 50mm apertures. These large DC levels distort the data read from the three apertures. The data presented here was taken prior to the integration of additional filtering and baffling.

In many point-to-point lasercomm systems, large divergence beams are transmitted to minimize the impact of beam wander due to atmospheric fluctuations. With the integration of a fast steering mirror into our transmitter configuration, we have the ability to transmit at best collimation and easily adjust for pointing changes after noticeable beam movement. Although optical transmit power is conserved when the transmitter divergence is narrow, any uncompensated beam wander may affect the integrity of the three aperture voltage measurements being logged. To characterize the impact of beam motion on the three apertures, measurements were made over a variety of power levels and divergences. A single-axis translation stage allows the divergence of the transmit beam to be manually changed. The three aperture voltage data shown in Fig. 7 was acquired at best collimation, with a transmit power of 20 dBm during a 30 minute period. In Fig. 7a the beam was intentionally pointed off-axis, while the link was realigned and centered on-axis before acquiring the data in Fig 7b.
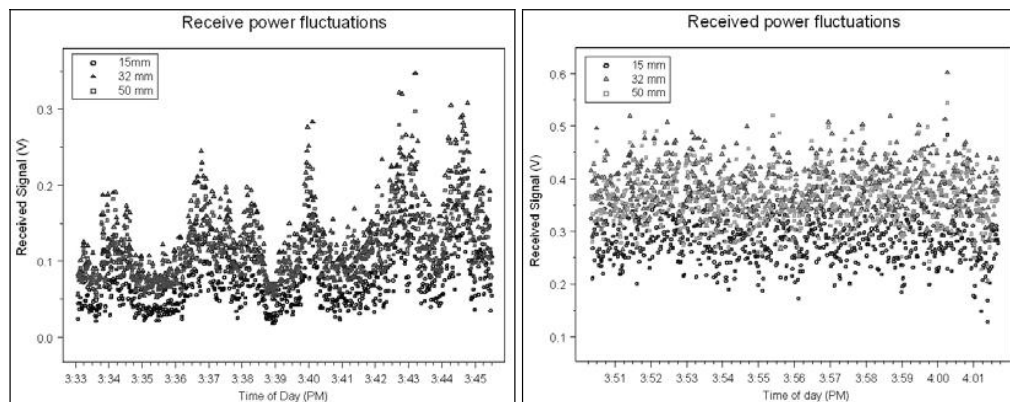

Fig. 7 a,b: Samples of voltages measured off of the 15mm, 32mm, and 50mm apertures. Fig. 7a(left) shows significant voltage fluctuations due to beam wander in the transmitter beam at best collimation, with the beam intentionally aimed off-center. Fig. 7b(right) is a sample the beam was centered on the receivers, and the impact of beam wander is minimized during the acquisition.

The correlation coefficients for the data presented in Fig. 7a and 7b are presented in Table 1. The correlation coefficients are calculated using a signal with a mean of 0. Since the TAAPD receiver voltages are averaged over 1 second intervals, only low frequency correlations are presented here. The received power measurements shown in Fig. 7a are highly correlated. The data presented in Fig. 7b appears to have maintained pointing with the divergence set to best collimation. The correlation coefficients between the apertures are nearly 15% lower, indicating a weaker component of the correlation due to beam motion.

Apertures→	15mm – 32mm	32mm – 50mm	15mm – 50mm
Fig 7a data	0.9914	0.9950	0.9969
Fig 7b data	0.8308	0.8576	0.8648

Table 1: Correlation coefficients of the data presented in Figs. 7a and 7b.

In addition to assessing the impact of beam wander on the three aperture setup, measurements were made at various transmitter power levels and divergences (z-positions). Fig. 8 shows the correlation coefficients of the apertures at transmitter output power levels ranging from 20 dBm to 34.7 dBm. The TAAPD detectors did not saturate during the acquisition. The correlation coefficients are concentrated in the range of 0.85 to 0.925, and as expected, do not display a significant power dependence. The data was taken during a 10 hour period.
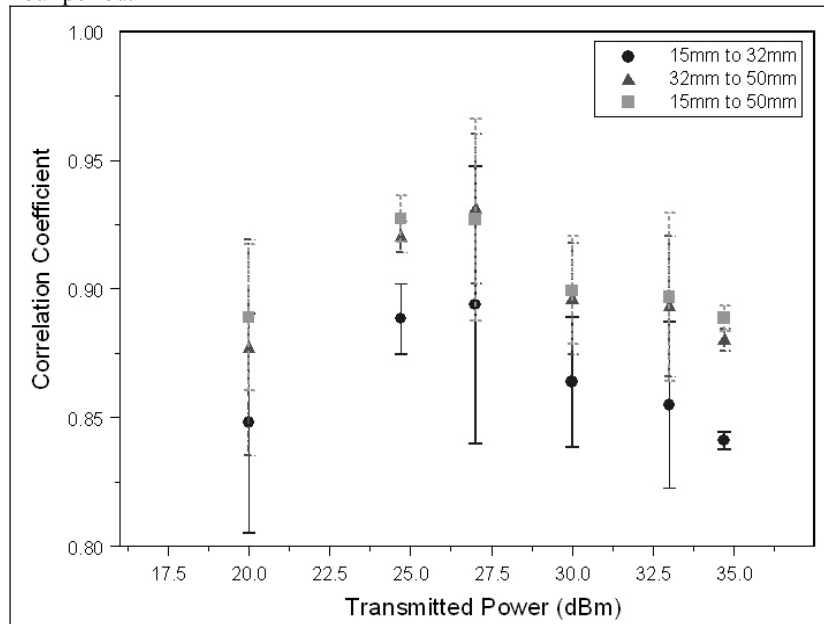

Fig. 8: Correlation coefficients for different aperture pairs in the three aperture setup. The voltage readings off the apertures are highly dependent. A strong power dependence is unclear.

The correlation coefficients of the logged voltage averaged over 1 second intervals is plotted against divergence in Fig. 9. At large divergences, a decreased correlation coefficient is expected since the effects of beam motion are minimized when the beam size is large compared to the receiver size. There is a trend of decreasing correlation coefficients in Fig. 9, however, at best collimation the coefficients are significantly lower than expected.
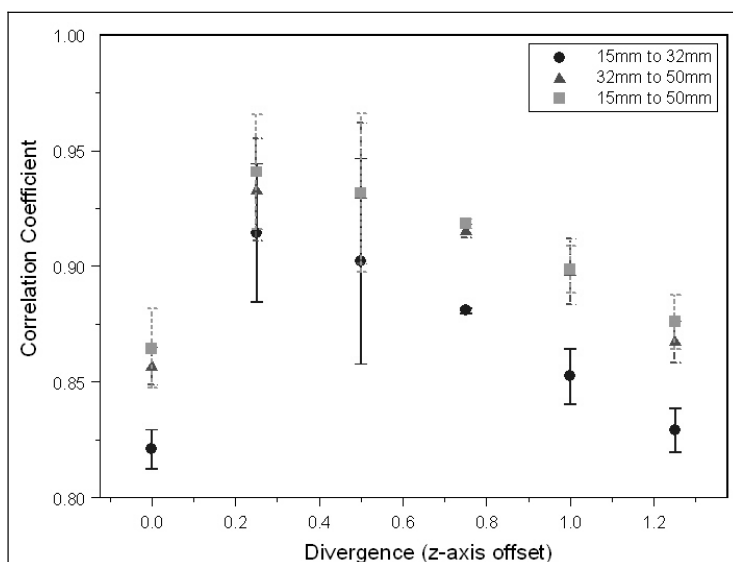
Fig. 9: Correlation coefficients for the correlation of the received signal. At x=0, the beam is at best collimation, resulting in a divergence of ~100µrad (full angle). At x=0.5, the divergence is approximately 500µrad to 600µrad (full angle).

The scintillation index was calculated from the acquired three aperture data using the equation:

$$\frac{\sigma^2_{Data} - \sigma^2_{BG}}{\left(\mu_{Data} - \mu_{BG}\right)^2} \qquad (2)$$

where σ^2_{Data} and μ_{Data} are the variance and mean of the logged voltage of each aperture over a 1 minute interval. The background variance and mean, σ^2_{BG} and μ_{BG}, were acquired before or after each data set. The scintillation indices for the data in Fig. 7a and 7b are shown in Fig. 10a and 10b. The scintillation indices for pairs of apertures (32mm vs 15mm, 50mm vs 32mm, and 50mm vs 15mm) are plotted in Fig. 11a and 11b. If the aperture pairs are strongly correlated, it is expected that the scintillation index of one aperture with another will be positive and increasing with scintillation index, σ^2_I.
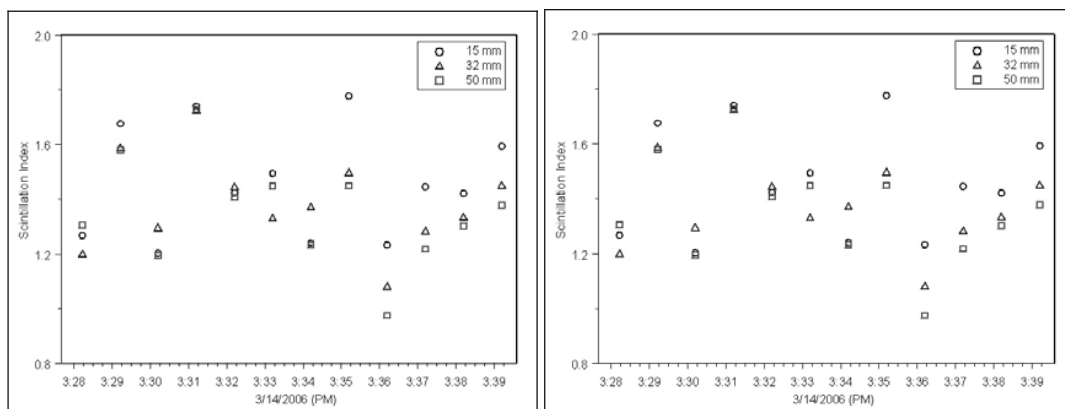

Fig. 10a (left) and 10b (right): The scintillation index is plotted for the data in Figs. 7a and b.
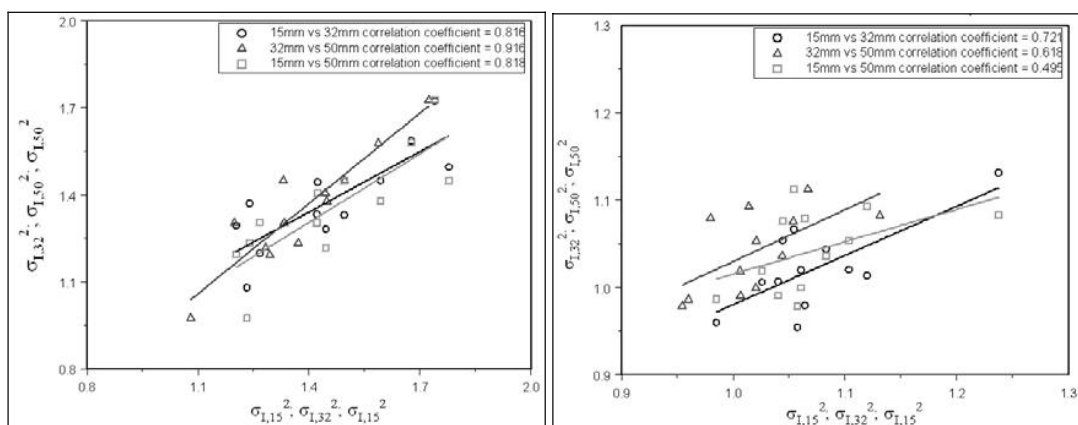
Fig. 11a (left) and 11b(right): The correlations of the scintillation index for the 15mm, 32mm, and 50mm apertures. The data on the right is less strongly correlated.
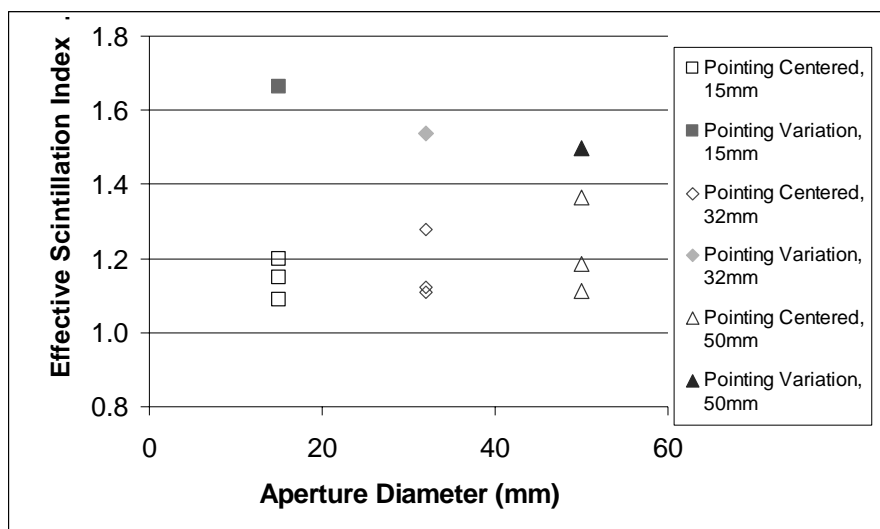

Fig. 12: Effective scintillation index for the three different apertures when the beam was intentionally pointed off-axis (pointing variation), and when the beam was centered on-axis (pointing centered). The data from Fig. 7 was used.
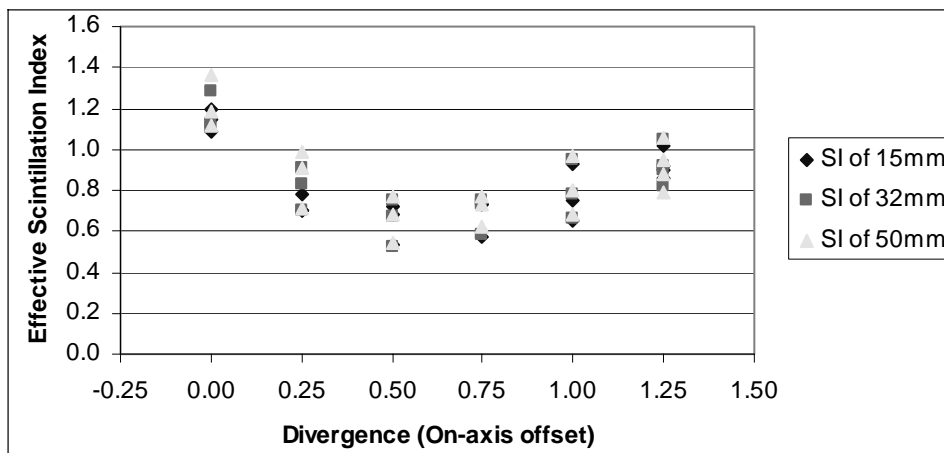

Fig. 13: Effective scintillation index as a function of beam divergence.

From Fig. 11b, apertures that are closer in size (ie. 15mm and 32mm, 32mm and 50mm) appear to show stronger correlations than relationship between the smallest and largest aperture. An increased amount of aperture averaging on the 50mm aperture reduces the correlation of the 50mm aperture with the 15mm aperture, as expected. In Fig. 11a, there is a substantial component of the correlation that is due to the beam motion. The spread of the data in Fig. 11 b indicates that the data is less strongly correlated. Fig. 12 shows the measured effective scintillation index, which includes the effects of beam wander, as a function of the TAAPD aperture diameter. When the pointing was intentionally moved off-axis, the measured scintillation index was significantly higher than the properly aligned values. Beam wander has a strong effect on the measured three aperture data, so care must be taken to ensure that measurements are accurately quantifying the atmospheric fluctuations.

In Fig. 13, the effective scintillation index is plotted as a function of beam divergence. The scintillation index should be stronger at lower divergences, since there is a significant component due to beam motion. As the divergence is increased, the scintillation index should plateau. From Fig. 13, the effective scintillation index drops by a factor of two as the divergence is increased from ~100μrad to ~500μrad. As the beam diverges further, the effective scintillation index increases, which is likely due to a lower signal-to-noise ratio. The lower signal-to-noise is caused by the decreased intensity at larger divergences, resulting in lower voltages on the TAAPD detectors. At best collimation, the TAAPD dectectors read values in the 1V range, while at widest divergence readings are in the low 10s of mV, with background levels near ~1mV. The data points at a given divergence in Fig. 13 represent different transmitter output powers.

FUTURE WORK

Adjustments will be made to the Tilghman Island setup to improve the quality and accuracy of the optical propagation measurements. The three aperture setup will continue to be improved as necessary. The addition of 1550nm filters should help prevent the background light levels from affecting the measurement data. The data will then be used to determine inner and outer scale and C_n^2 using the method in Ref. 4. The coherent scintillometer will also be compared to the incoherent scintillometer.

CONCLUSION

Data to support the characterization of free space optical communication in the maritime environment is presently being collected. The data presented here is a preliminary analysis of the accuracy of the three aperture setup and angle-of-arrival monitor. The angle-of-arrival monitor appears to be insensitive to beam divergence and power (within the limited dynamic range of the CCD) and gives a consistent indication of turbulence strength. The TAAPD monitor is being improved to give a better indication of atmospheric parameters uncorrupted by background light and beam wander. Improved filtering and baffling along with measuring correlated versus uncorrelated components of the TAAPD voltage fluctuations are some of the improvements being investigated.

ACKNOWLEDGEMENTS

REFERENCES

[1] Stell, Mena, et al., "Passive optical monitor for atmospheric turbulence and windspeed," Proceedings of the SPIE: Free-Space Laser Communication and Active Laser Illumination III, vol. 5160, July 2004, p. 422-431.

[2] Andrews, Larry C., Ronald L. Philips, and Cynthia Y. Hopen, *Laser Beam Scintillation with Applications*, SPIE Press, 2001.

[3] Suite, Michele, et al. Proceedings of SPIE: Atmospheric Propagation III This volume, April 2006.

[4] Vetelino, Frida Strömqvist, et al., *Proceedings of SPIE: Atmospheric Propagation II*, vol. 5793, April 2005.

[5] Moore, C. I., et al. "Atmospheric Turbulence Studies of a 16 km maritime path," Proceedings of the SPIE: Atmospheric Propagation III, Vol, 5793, pg 78-88, April 2005.

[6] Hooper, W.P., G.E. Nedoluha, and L.U. Martin, "Retrieval of near-surface temperature profiles from passive and active optical measurements," **Optical Engineering**, vol. 41, no. 7, July 2002, p. 1586-1602.